

Examination of Precursors in Fly Ash for Development of an Engineered Geopolymer Concrete

Fernando Soto¹, Milap Dhakal², Kunal Kupwade-Patil², Daniela S. Mainardi¹, Erez N.Allouche²

¹Institute for Micro-manufacturing, Chemical Engineering, Louisiana Tech University, Ruston, LA 71272

²Alternative Cementitious Binders Laboratory (ACBL), Louisiana Tech University, Ruston, LA 71272

ABSTRACT

Pore structure of Geopolymer Concrete (GPC) is of importance and depends on the pore network and microstructure. The current study examines atomic, micro and macroscale properties of GPC prepared from the vital precursors, which influence the mechanical properties of Geopolymer Concrete (GPC). Despite significant experimental and theoretical efforts which have been made recently to elucidate the exact mechanism that governs the polymer reactions in geopolymers, it still remains a challenging task to this date. Knowledge of processes such as hydration (adsorption of relevant species) and dissolution (release of Si/Al species) and their interaction at the molecular level is essential to understand and manipulate the physicochemical properties of geopolymer precursor materials (e.g. albite). This work undertook a computational approach utilizing density functional theory calculations to study the effect of NaOH alkaline solutions on the surface of albite followed by experimental observations. Geopolymer Concrete specimens were batched using the fly ashes which consisted of these precursors such as albite, labradorite and anorthite. XRD analysis was conducted to examine the effect of crystalline to amorphous ratio which contributed to the mechanical strength of geopolymer concrete (GPC). Internal pore structure was examined using high resolution X-Ray Microtomography (μ CT) and the pore network was studied for both low and high strength geopolymer concretes. μ CT studies revealed that the particle size distribution (PSD), type of precursor, fly ash consumed in the geopolymerization and crystalline to amorphous ratio had significant impact on the pore structure and the microstructure properties of the hardened geopolymer concrete.

1. Introduction

1.1 Background

The geopolymer structure was first described by Joseph Davidovits in 1978 as a non-crystalline or quasicrystalline gel that has a three-dimensional framework ¹. This geopolymer is a polymerized material consisting of natural minerals; particularly, an Al-

O-Si network structure, in which the Si-O tetrahedron and Al-O tetrahedron are alternately bonded through oxygen atoms^{2, 3}. Geopolymers are made by adding aluminosilicates to concentrated alkali solutions for dissolution and subsequent polymerization to take place⁴. Such a distinctive structure makes it possess favorable characteristics, featuring high strength, elevated temperature resistance, rapid hardening property, insulation, resistance to acid and corrosion, and ability to encapsulate/immobilize hazardous and radioactive materials⁴⁻⁶. Thus, leading to high performance in broad applications such as transportation, emergency repair, and solid waste disposal^{7, 8}. Ultimately, the alternative to Portland cement in the 21st century⁹. In spite of these major advantages, the widespread use of geopolymers is limited due to lacking long term durability and incomplete scientific understanding.

Currently, key raw materials for making geopolymers include aluminosilicate precursors-fly ash, clay, kaolin, granulated blast furnace slag and industrial solid waste material^{10, 11}. Combining the reactive aluminosilicate precursors to alkaline/silicate solutions (NaOH, KOH), leads to dissolution, polymerisation and solidification of the materials¹². Due to these complex reactions that occur in all the different precursor materials, the structure and morphology of geopolymers are poorly understood. This means that the exact details of the polymerization process depends on the individual ash source selected and that no two exactly the ashes will follow the same mechanism¹³. Moreover, many of the aforementioned processes occur to some degree simultaneously, making the in-situ characterization of the different processes challenging¹⁴. This elucidation can be achieved through integrated computational and experimental studies. These studies will help us understand and develop the physics, chemistry, materials and processing that are necessary to develop a new design mix to achieve considerable societal benefits. In this work, we have undertaken a computational approach utilizing density functional theory to compute the interaction energy at the interface of NaOH alkaline solution and a (001) albite surface. This paper is organized as follows. In Section 2 we briefly describe the methodology employed. Section 3 contains the results and discussions. Conclusions follow in Section 4.

1.2 Computational Literature Review

Previous investigations on modeling the geopolymerization process have elucidated decisive reaction details; however, an in-depth knowledge of the physicochemical properties of all the atomistic processes occurring during geopolymerization is still lacking¹⁴. In this regard, the influence of alkaline activators on geopolymer and glassy material has received considerable attention^{6, 15, 16}. It has been found that properties of fly-ash geopolymer concrete are significantly altered by the presence of alkaline activator solutions¹⁷. The alkaline activator solutions can inhibit (improve) the facet growth rate and modify the geometry of aluminosilicate precursors; thus, interfering (promoting) the polymerization steps^{11, 18}. In view of the above, herein, the focus of interest for this paper lies primarily in the interaction energy of the aluminosilicate minerals with the NaOH/H₂O (H₂O is treated implicitly in these models) liquid interface. Previous modeling work at the solid-liquid interface was devoted to validating the use of density functional theory (DFT) by analyzing structural data of clay minerals^{19, 20}.

Morrow et al. studied the reactions of aluminosilicate clusters with water using ab initio calculations. Particularly, the computational work showed that Al species from protonated and neutral Al-O_{bridge}-Si sites can leach before Si species, matching available experimental data ²¹. Moreover, Bandura et al. performed plane wave DFT calculations to study the atomic structure, preferred H₂O adsorption sites, adsorption energies, and vibrational frequencies for water adsorption on the R-quartz (101) surface ²². Bandura and co-workers concluded that the maximum adsorption energy is found for a single H₂O molecule adsorption in the 1×1 surface cell ²². Moreover, addition of cations (Na) to charge balance molecules strongly affects geometry and dissolution mechanisms of mineral surfaces ²³. More recently, White et al. has utilized first principles calculations and kinetic modeling to study the atomistic structure of key precursor materials such as metakaolin and kaolinite²⁴⁻²⁶.

Xu and co-workers used wavefunction-based ab-initio methods to revise the dissolution mechanisms of Al-Si minerals in highly alkaline solutions²⁷. Aluminum atoms break more readily than silicon, significantly influencing the dissolution energy ¹¹. Provis et al. developed a reaction kinetic model consisting of various mathematical modeling techniques, such as statistical thermodynamics and pair distribution functions ²⁸. A statistical thermodynamic model was used to describe the Si/Al ordering within the tetrahedral aluminosilicate gel framework. This kinetic model briefly described the raw material dissolution and combination of amorphous and zeolite precursor gel networks. The model results were compared to the calorimetric and EDXRD data, providing information on gel chemistry and the framework for understanding the behavior of geopolymer-forming phases. However, an approach to understand the properties of precursor materials is needed to obtain accurate knowledge pertaining to their microscopic structure via advanced experimental and molecular modeling techniques ²⁹. Despite the limited research that has been conducted on modeling the geopolymerization process of alkali activated cements, details regarding accurate molecular level mechanistic information has to be understood in depth. The experimental results obtained within the research group would be useful to examine the predictive nature of molecular modeling.

2. 1 Experimental Procedure

Geopolymer concrete was prepared with six different fly ashes. The chemical composition of the fly ashes obtained via X-ray fluorescence (XRF) spectroscopy is shown in Table 1. GPC mortar samples were prepared in accordance with ASTM C-305. GPC mortar cubes of size (2in×2in×2in) were prepared using commercially available sodium silicate and freshly prepared sodium hydroxide (14 M NaOH). The activator to binder ratio in the range of 0.4-0.9 was used in the preparation of geopolymer concrete. The samples were subjected to a thermal curing at 140±5 °F for the period of 72 hours. GPC specimens were subject to compression test as per ASTM C109, after three days heat curing. In addition, microstructure studies along with pore structure analysis was conducted using X-Ray fluorescence spectroscopy (XRF), X-ray diffraction (XRD), X-ray microtomography (X-Ray μCT) and mercury intrusion porosimetry (MIP).

Table 1. Chemical composition of fly ash

No	FA Code	Chemical Composition (%)							
		SiO ₂	Al ₂ O ₃	CaO	Fe ₂ O ₃	MgO	SO ₃	Na ₂ O	K ₂ O
1	DH	58.52	20.61	5.00	9.43	1.86	0.49	0.52	-
2	SJ2	56.39	27.36	4.69	3.34	0.75	0.26	1.50	0.95
3	PK	59.25	18.43	9.23	5.61	3.23	0.35	0.50	1.63
4	NE	31.26	19.76	28.53	6.47	4.81	1.45	2.27	0.47
5	HW	33.38	14.72	26.80	7.69	1.49	10.36	0.56	0.79
6	MO	55.61	19.87	12.93	4.52	2.49	0.49	0.67	0.86
7	IL1	53.00	25.88	3.34	9.45	1.70	0.20	0.71	2.23

2. 2 Computational Approach

To study the interaction of alkaline solution NaOH and H₂O (treated implicitly) with a (001) facet of aluminosilicate mineral (e.g. albite), an approximation comparable to surface docking was developed to calculate the energy of interaction. The basis of this approach is to analyze the interaction energy between the NaOH molecules and the individual (001) facet, which is cleaved from the appropriate crystal structure. If the molecules have a preferred interaction with an aluminosilicate, the facet growth of this mineral will be slower. Thus, the other fast-growing surfaces will vanish, and eventually, the slow-growing aluminosilicate surface will become dominant during the polymerization process. In this paper, we utilized a slab model approach for the aluminosilicate mineral, comprised of two layers of approximately 6 Å thick and a vacuum region of approximately 25 Å normal to the surface to avoid interaction of periodic images. For the sake of simplicity, NaOH molecules were only placed at the center of the slab. The present work is a first-step approach in developing a one-step "just add water" geopolymer design mix. This is done by comparing the interaction energy of a NaOH alkaline solution with several aluminosilicate minerals, and the result for albite is presented here.

The DFT study of NaOH/H₂O interaction with slabs of aluminosilicate minerals has been performed using the DMol₃ package in the Materials Studio® software of Accelrys³⁰. For all geometry optimizations, we used a double numerical basis set with d polarization (DND) within the local density approximation with Perdew-Wang exchange-correlation functional (LDA/PWC). Single-point energy calculations were performed within the generalized gradient approximation (GGA), and Perdew, Becke and Erzenhorf exchange-correlation functional (PBE) with a larger basis set (DNP). Energies with both basis sets were compared to estimate the influence of basis sets in the interaction energy. As mentioned previously, slabs of (001) facet were constructed by cleavage of the unit cell structures (see figure 1). The sampling of the reciprocal *K*-points was generated at the gamma point only, considering that the slab models are large enough. In this work, the DMol-COSMO method is applied with periodic boundary conditions³¹. This method is suitable for the solid-liquid interfacial energy calculations between a surface and an idealized dielectric liquid with a dielectric constant value of 78.54 to reproduce a neutral pH value of 7. Moreover, the water in a geopolymer concrete mixture plays no role in the chemical reactions that take place at the interface, making this method suitable for aluminosilicate minerals, as well³². Finally, the

computational model represents a 0.40 alkaline solution/surface ratio, which is standard in the geopolymer industry^{33, 34}.

3. Results and Discussion

Compressive strength for GPC prepared with 7 different fly ashes and porosity obtained via Mercury intrusion porosimetry is shown in Figure 1. GPC prepared with IL exhibited the maximum strength of 69 MPa and a minimum porosity of 3 %, while HW exhibited minimum strength of 4 MPa, and a porosity of 16 %. A significant variation in strength and porosity were observed among geopolymer concrete specimens prepared with Class C and F fly ashes. The variation in strength could be attributed to various factors such as particle size distribution of the fly ashes, the crystalline and amorphous content of the fly ash and GPC, along with the overall pore structure of geopolymer concretes.

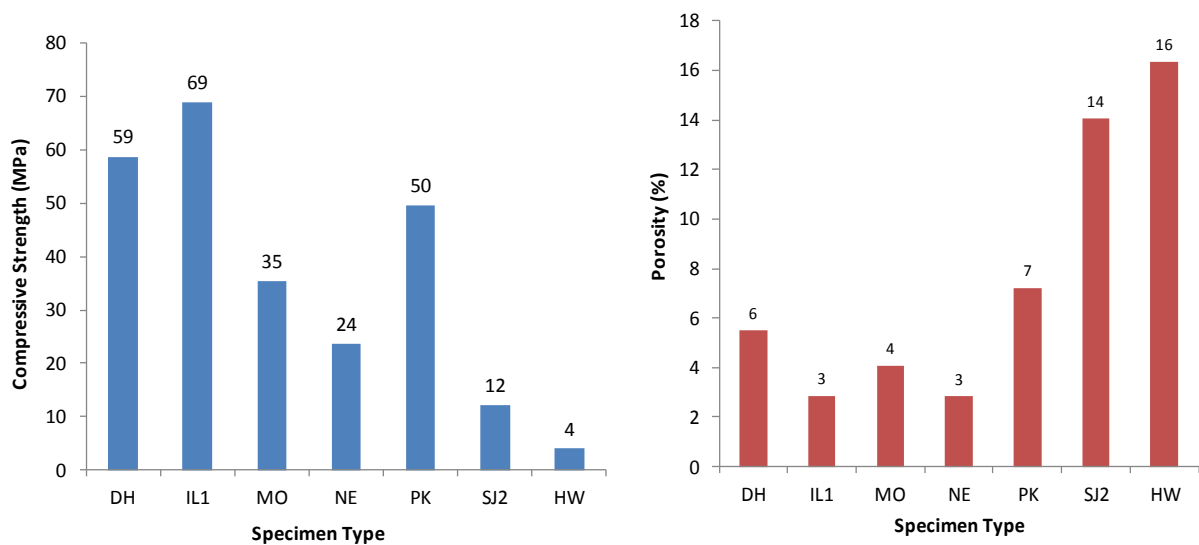


Fig 1. Compressive strength and porosity analysis of geopolymer concretes

The compressive strength versus ratio of $(\text{SiO}_2 + \text{Al}_2\text{O}_3)/\text{CaO}$ is shown in Figure 2. The compressive strength values of GPC specimen NE, MO, DH and IL increase with the ratio of $(\text{SiO}_2 + \text{Al}_2\text{O}_3)/\text{CaO}$. The specimens HW, PK and SJ2 also exhibited this trend but the strength increase was much lower as compared to NE, MO, DH and IL. The parameters such as SiO_2 , Al_2O_3 and CaO are not sufficient to provide an accurate relationship which can be used to design an engineered geopolymer concrete. In addition, parameters such as crystalline phases which are responsible for the formation of N-A-S-H system studied via XRD and the overall pore structure using MIP and X-Ray μCT was used to engineer the geopolymer concrete.

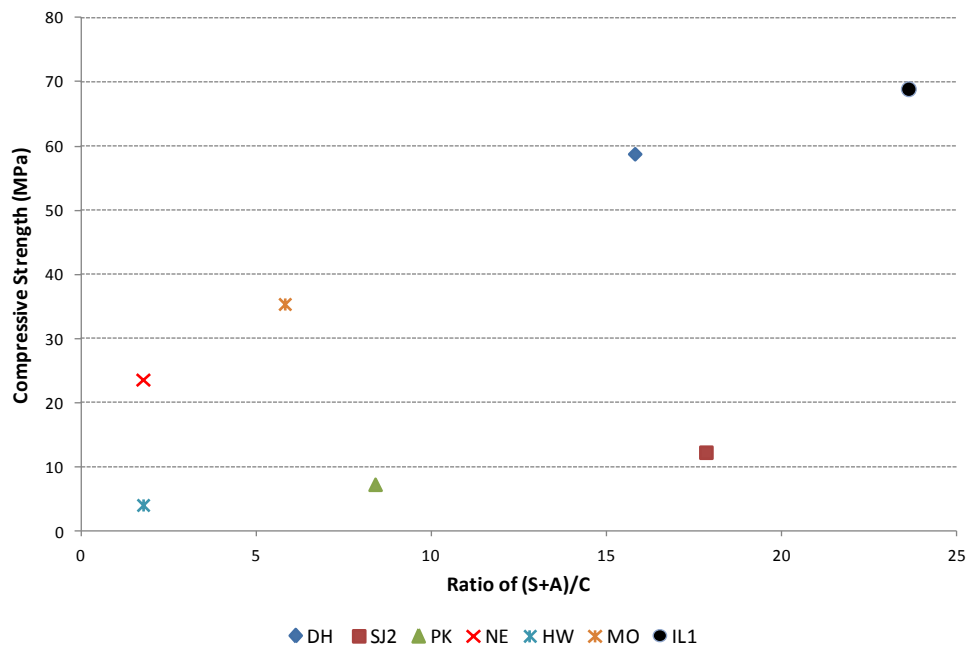


Fig 2. Ratio of $(\text{SiO}_2 + \text{Al}_2\text{O}_3)/\text{CaO}$ versus compressive strength

The activator solution required to prepare GPC is related to PSD, which is one of the parameters that can be used to engineer GPC. Higher the PDD (meaning larger FA particles) greater amounts of activator solution will be required to alkali activate the fly ash. Relationship between PSD, AC/FA ratio along with the compressive strength of GPC's is shown in Figure 3. GPC prepared with HW fly ash exhibited the least compressive strength (4MPa), while demonstrating a 76% of the particle finer than 45 μm . In contrast, GPC (IL) showed a maximum compressive strength of 69 MPa, with its precursor fly ash having 71% of its particles finer than 45 μm . In addition, GPC NE exhibited a lower compressive strength of 24 MPa, with the finest particles (86% passing 45 μm), this trend contradicts the concept that finer the fly ash particles, higher is the mechanical strength. The fly ash SJ2 had a PSD of 58% passing through 45 μm and thus it required a high AC/FA ratio of 0.94 to prepare the GPC specimen, to maintain consistent workability. In contrast, HW fly ash exhibited a PSD of 86% passing through 45 μm , although the fly ash had fine particle size, it required larger content of activator content (AC/FA =0.85) to activate the fly ash for its geopolymerization. CaO content of SJ2 and HW fly ashes are 4.69% and 26.80 %, respectively. HW fly ash had higher CaO content by a factor of ~7 when compared to SJ2 fly ash.

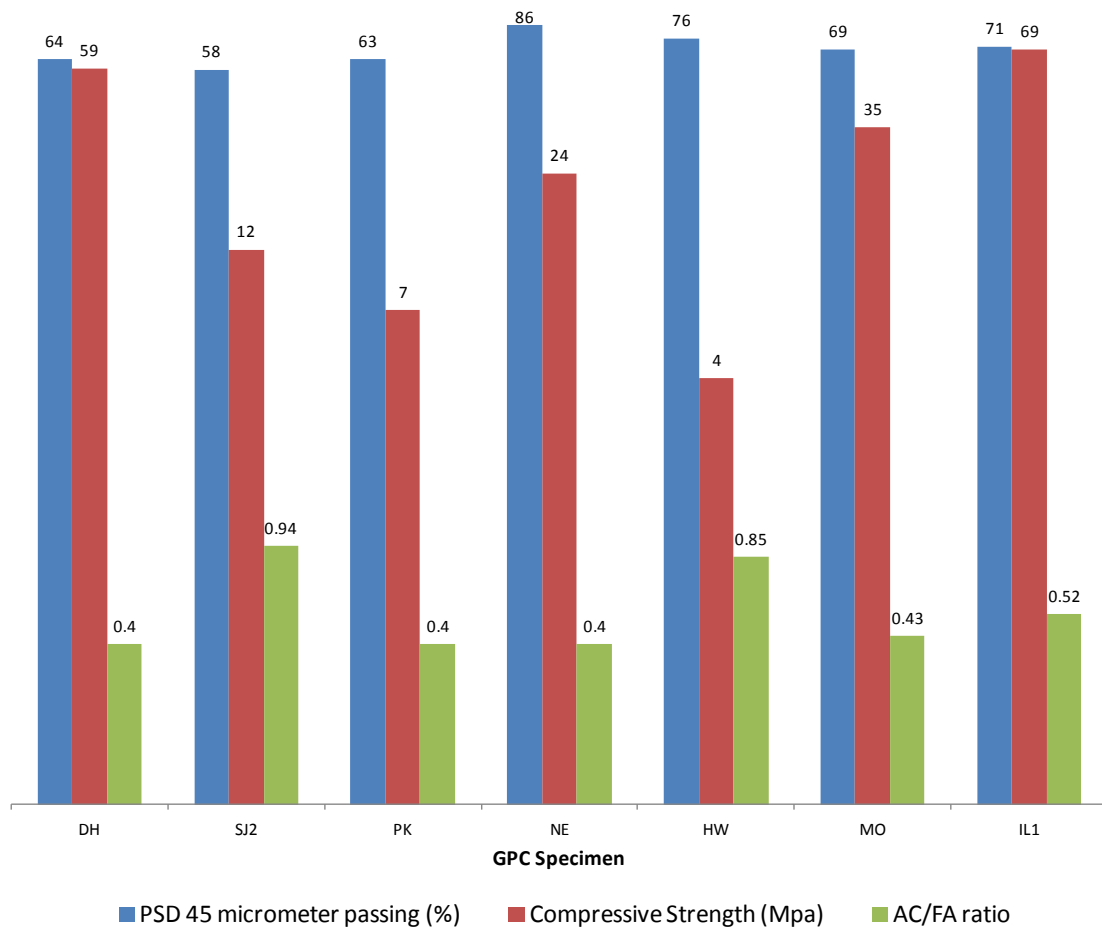


Fig 3. Relationship with Particle size distribution (PSD) and compressive strength of GPC

This indicates that CaO content plays a crucial role in determining the workability of the mix. Higher CaO content in the FA precursor shortens the setting time and also requires higher AS/FA ratio in order to maintain the workability of the GPC mix, which consequently leads to reduction in its characteristic strength. The CaO present in the fly ash needs to be involved in the formation of N-A-S-H and C-A-S-H network, which is responsible for strength gain in geopolymer concretes. If excess CaO is present in the fly ash and is not involved in the geopolymerization network, it could remain in the unreacted state in the cement matrix, which could contribute to the reduction in strength. Further studies are required to establish a relation to correlate the reduction in strength, with the increase in CaO content of the fly ash.

XRD analysis of GPC's with low (4 MPa), medium (35MPa) and high strength (69MPa) geopolymer are shown in Figure 4. High strength (IL1= 69MPa) and medium strength GPC (MO) exhibited phases such as hydrosodalite, albite, mullite and quartz, while low strength GPC (HW) showed weak peaks of albite and mullite. The albite and hydrosodalite peak could be attributed to strength forming phases which form the crystalline phase of the N-A-S-H system^{35, 36}. The precursors in the fly ash such as

albite, sodalite and stalbite may also contribute to strength, if significant quantity of crystalline phase is detected after the alkali activation of the fly ash. This shows that certain strength forming crystalline phase play a crucial role in developing and engineering the strength of Geopolymer concretes.

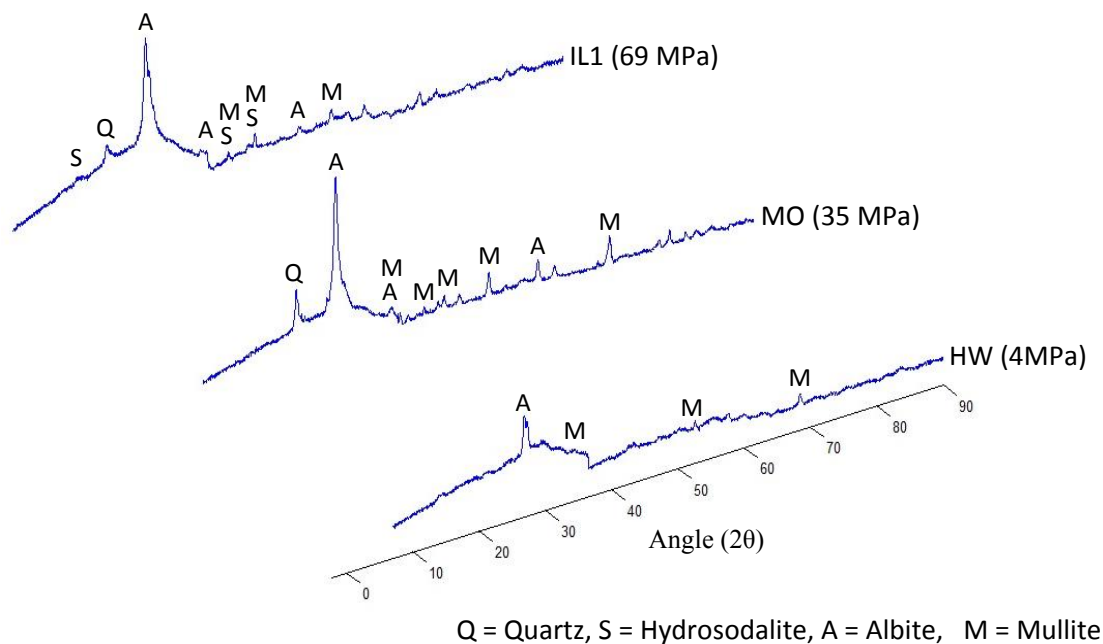


Fig 4. XRD analysis of low (4 MPa), medium (35 MPa) and high strength (69 MPa) geopolymer concretes

X-Ray μ CT of low (GPC-HW), medium (GPC-MO) and high (GPC-IL) strength GPC is shown in Figure 5, 6 and 7 respectively. GPC prepared with HW fly ash exhibited the least strength (4MPa) and the pore structure studies show a clear distinct cracking along with large voids sizing in the range of 4000-6000 nm. GPC-MO exhibited voids in the range of 3000-4000 μ m, with a compressive strength of 35MPa. The GPC-IL exhibited a maximum strength of 69 MPa with a pore size ranging from 800-1000 μ m, with no signs of cracking. This shows that analysis of pore structure helps in understanding the mechanism of voids and the connectivity of the pores. Further studies are required to quantify the tortuosity of the pore network and to provide a relationship between pore sizes and compressive strength. This study indicates that not only the physical parameters such as PSD, crystal structure, CaO and AC/FA are sufficient to engineer the GPC, rather the overall pore structure, precursor of the fly ash and particular crystalline phases (albite and hydrosodalite) which form the N-A-S-H system play a important role in designing geopolymer concretes.

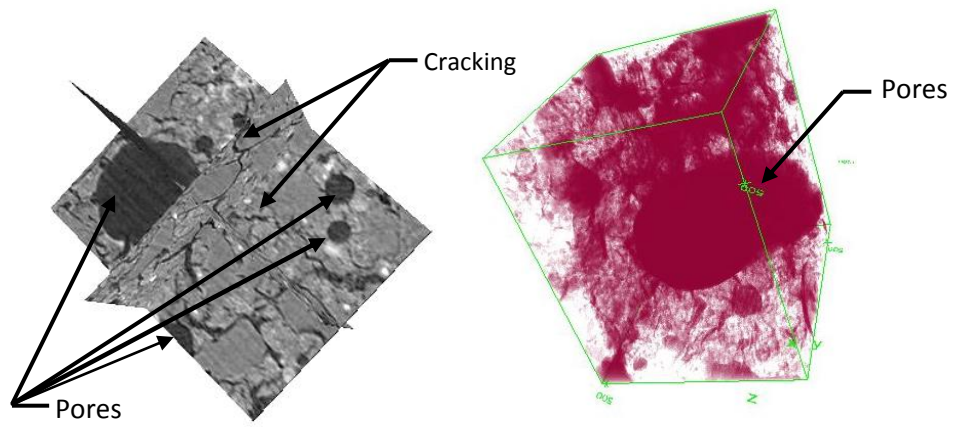


Fig 5. (a) Orthoslice image of GPC (HW), (b) 3D image exhibiting the large pores

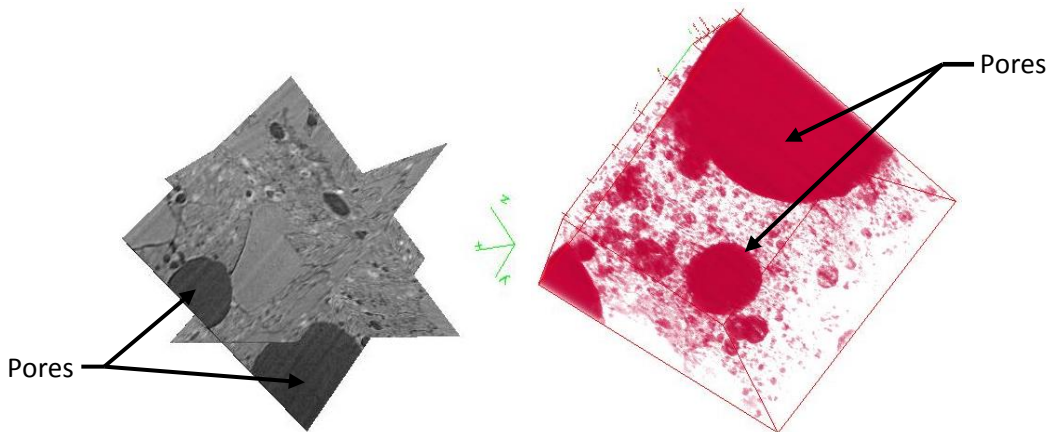


Fig 6. (a) Orthoslice image of GPC (MO), (b) 3D image exhibiting the pores

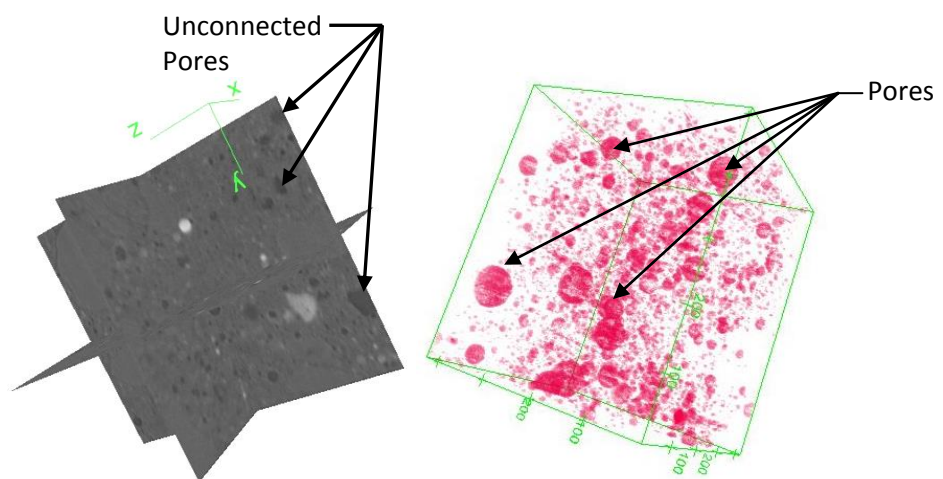


Fig 7. (a) Orthoslice image of GPC (IL), (b) 3D image exhibiting the pores

3.1 Unit Cell

The aluminosilicate mineral considered as representative of a geopolymer precursor is shown in Figure 8. The following calculations use this model as input structures for the slab models.

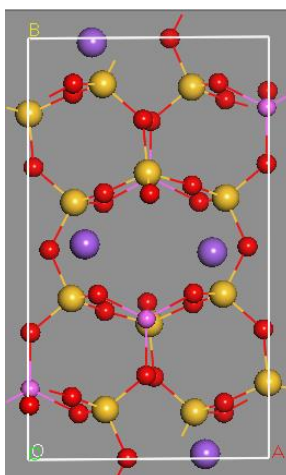


Fig 8. Optimized structure of Albite ($\text{NaAlSi}_3\text{O}_8$) crystal structure, showing silicon (yellow), oxygen (red), aluminum (pink) and sodium (purple) atoms.

The lattice parameter for albite is shown in Table 2. Optimization of the albite unit cell geometry within LDA leads to $a = 8.096 \text{ \AA}$, $b = 12.823 \text{ \AA}$ and $c = 7.353 \text{ \AA}$. The calculated volume of the unit cell is slightly larger than the experimental value by less than 2 %. This is common for molecular crystals and a known limitation of DFT calculations³⁷. The LDA functional describes more accurately the structural parameters of the albite crystal than the Generalized Gradient Approximation (GGA), therefore, all the calculations in this paper are done at the local density approximation level.

Table 2 Optimized structural parameters of Albite

Model	Lattice Parameter (\AA) at LDA Theory Level	Lattice Parameter (\AA) at GGA Theory Level	Experimental Lattice Parameters (\AA)	Free Volume at LDA Theory Level	Binding Energy (eV)
Albite	$a = 8.096$ $b = 12.823$, $c = 7.353$	$a = 8.234$ $b = 13.104$, $c = 7.409$	$a = 8.115$ $b = 12.762$, $c = 7.157$	10.06%	-329.714

The binding energy of a precursor material is a vital parameter to determine the reactivity for geopolymerization³⁸. Table 1 shows that the binding energy of the albite crystal is rather high at a value of approximately -330 eV, where, the binding energy reported in DMol₃ is to dissociate the crystal into atoms at infinite separation. Therefore, the binding energy of species such as Si and Al needs to be calculated separately (as they provide insights into leaching processes). The free volume within a precursor material may also be responsible for the propensity of precursor material to undergo

geopolymerization. For the albite crystal, a tool within Materials Studio® was used to generate the necessary Van der Waal surfaces (VdW) to calculate the free volume. The VdW surfaces were created by using a default atom-probe to pass through the structure³⁹. The albite crystal (see Figure 9) shows a free volume percentage of approximately 10%. This percentage value is in accord with the percentage values of similar precursor materials⁴⁰.

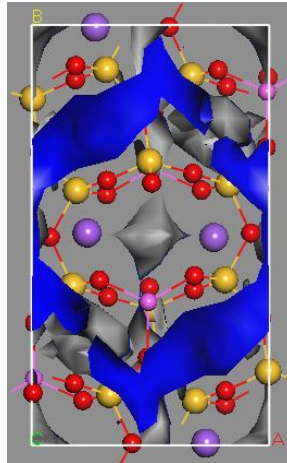


Fig 9. Optimized structure of Albite ($\text{NaAlSi}_3\text{O}_8$) crystal structure with voids shown in blue and occupied volume shown in a darker gray

3.1.1 Electronic Structure of Unit Cell

Electron density maps are constructed applying DFT calculations as implemented in the Materials Studio® package, utilizing the aforementioned unit cell as the input structure. The valence electron density (see Figure 10) is obtained by mapping field values onto colors for volumetric objects. Particularly, a slice view was adopted on 32 color bands with zero (blue) representing electron-deficient zones and 32 (red) representing electron-rich zones.

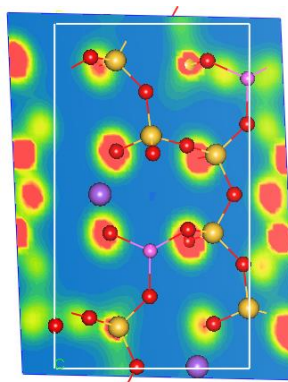


Fig 10. Electron Density Map of Albite as seen from the [001] direction

A (001) slice through the valence charge density of the albite unit cell allows for visualization of the valence charge distribution at the LDA approximation. Red colored

areas around O atoms indicate a higher electron density around these atoms and explained by their higher electronegativity value (3.5) when compared to Si (1.8) and Al (1.5). This trend is corroborated by a Mulliken charge analysis, showing O values ranging from -0.988e to -1.116e. Similarly, for Si and Al atoms the analysis shows charges between 1.918e and 1.807e, respectively. These implies the necessity of the presence of an alkali metal cation (Na) to create subunits of alternate Si and Al atoms to create a geopolymer structure.

3.2 Surface Model

The surface model construction can be divided into two steps. The first step is the surface construction and relaxation; and the second step is the simulation of the albite surface–NaOH interaction. The input for the surface model was the albite unit cell with parameters as listed in Table 1. Then, a self-consistent geometry optimization calculation was carried out in order to obtain the ground-state structure. Finally, the optimized structure was cleaved along the [001] direction to create an ideal surface. This results in a slab of 6 Å thickness and lengths 16.23 Å and 12.76 Å on *a*-direction and *b*-direction, respectively. Figure 11 exhibits the relaxed slab for albite. The surface relaxation energy is given by the difference between the energies after the last full relaxation and the first ionic relaxation.

$$\gamma = E_{\text{last}} - E_{\text{1st}} \quad (\text{Eq.1})$$

The surface relaxation energy is approximately 114 eV/system, which is rather high and will have an effect on the surface energy. Thus, the thickness of the slab may play an important role in determining the relaxation energies and interaction energies. Moreover, the binding energy of this model is -705.969 eV. To simulate the interaction energy, the albite surface-NaOH system was built setting the NaOH molecules model over the relaxed albite surface. Initially a nonbonding distance between the NaOH molecules and the surface was established, see Figure 11 b.

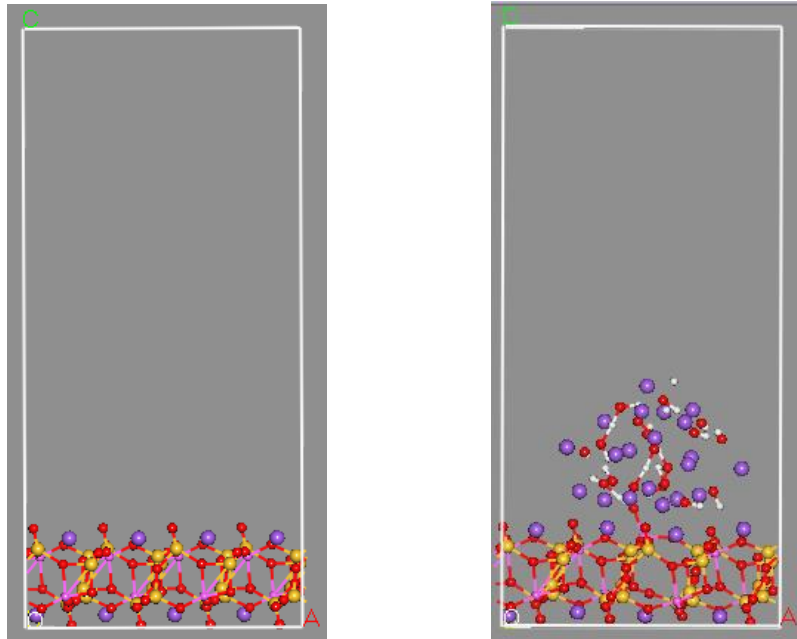


Fig 11. (a) Relaxed surface model for albite., (b) albite surface-NaOH system

Periodic boundary conditions were imposed, and all the atoms were allowed to relax. The electronic conditions for the LDA functional evaluation were conserved exactly in the same way as they were used for the surface generation. In order to clarify in a preliminary way the interaction energy between the molecules and the surface, a simple calculation of the NaOH molecules without the surface was carried out, see Figure 12. Twenty molecules of NaOH were enough to simulate a 0.40 ratio.

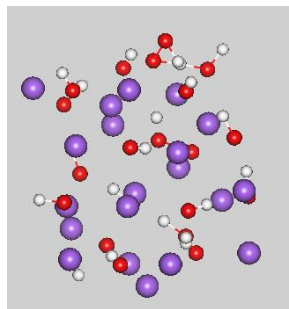


Fig 12. NaOH system modeled with COSMO

Following Eq.2, the interaction energy was calculated to be -167.62 eV which indicates a strong interaction. It is noteworthy that this interaction energy is strongly dependent of the surrounding solvent. Hence, it is necessary to perform a sensitivity analysis on the pH value of the solvent. This will be done through the continuum solvation model. It is also noteworthy that the binding energy of this system is -163.27 eV.

$$E_{\text{int}} = E_{\text{NaOH solution/surface}} - (E_{\text{alkaline solution}} + E_{\text{surface}}) \quad \text{Eq.2}$$

4. Conclusion

Geopolymer concrete was prepared with six different fly ashes. GPC were tested for compressive strength and microstructure analysis was conducted using XRD, while pore structure studies were done using MIP and X-Ray μ CT. This work shows that certain strength forming crystalline phase such as Albite and hydrosodalite play a crucial role in developing and engineering the strength of Geopolymer concretes. This study indicates that not only the physical parameters such as PSD, crystal structure, CaO and AC/FA are sufficient to engineer the GPC, rather the overall pore structure, precursor of the fly ash and particular crystalline phases (albite and hydrosodalite) which form the N-A-S-H system play a important role in designing geopolymer concretes.

This study also presents a computational study of an albite crystal, and a NaOH molecular model over the (001) albite surface. These models are analyzed through first principles calculations, and the ground state energies were obtained using the LDA approximation of the density functional theory. An attractive interaction was observed between the NaOH molecules and the albite surface. Finally, binding energies were computed, and a more exhaustive investigation of the Si atoms at Si terminated sites (called Si-O_{bridge}-Al to indicate the Si bond is broken from the O atom) and Al terminated sites (Al-O_{bridge}-Si to indicate that the Al-O_{bridge} bond breaks) is needed via quantum mechanical molecular dynamics. This is a first approach to determine the processes and energies leading to dissolution and leaching of the precursor species.

References

1. Davidovits, J., *Geopolymers*. Journal of Thermal Analysis and Calorimetry, 1991. **37**(8): p. 1633-1656.
2. Komnitsas, K. and Zaharaki, D., *Geopolymerisation: A review and prospects for the minerals industry*. Minerals Engineering, 2007. **20**(14): p. 1261-1277.
3. Provis, J.L., Lukey, G.C. and van Deventer, J.S.J., *Do Geopolymers Actually Contain Nanocrystalline Zeolites? A Reexamination of Existing Results*. Chemistry of Materials, 2005. **17**(12): p. 3075-3085.
4. Duxson, P., Provis, J.L., Lukey, G.C. and van Deventer, J.S.J., *The role of inorganic polymer technology in the development of 'green concrete'*. Cement and Concrete Research, 2007. **37**(12): p. 1590-1597.
5. Luna Galiano, Y., Fernández Pereira, C. and Vale, J., *Stabilization/solidification of a municipal solid waste incineration residue using fly ash-based geopolymers*. Journal of Hazardous Materials, 2011. **185**(1): p. 373-381.
6. Zheng, L., Wang, W. and Shi, Y., *The effects of alkaline dosage and Si/Al ratio on the immobilization of heavy metals in municipal solid waste incineration fly ash-based geopolymer*. Chemosphere, 2010. **79**(6): p. 665-671.
7. Ivan Diaz-Loya, E., Allouche, E.N., Eklund, S., Joshi, A.R. and Kupwade-Patil, K., *Toxicity mitigation and solidification of municipal solid waste incinerator fly ash using alkaline activated coal ash*. Waste management, 2012. **32**(8): p. 1521-1527.

8. Kupwade-Patil, K. and Allouche, E., *Impact of Alkali Silica Reaction on Fly Ash Based Geopolymer Concrete*. Journal of Materials in Civil Engineering, 2012.
9. Shi, C., Jiménez, A.F. and Palomo, A., *New cements for the 21st century: The pursuit of an alternative to Portland cement*. Cement and Concrete Research, 2011. **41**(7): p. 750-763.
10. Duxson, P., Fernández-Jiménez, A., Provis, J., Lukey, G., Palomo, A. and van Deventer, J., *Geopolymer technology: the current state of the art*. Journal of Materials Science, 2007. **42**(9): p. 2917-2933.
11. Xu, H., Van Deventer, J.S.J., Roszak, S. and Leszczynski, J., *Ab initio study of dissolution reactions of five-membered aluminosilicate framework rings*. International Journal of Quantum Chemistry, 2004. **96**(4): p. 365-373.
12. Fernández-Jiménez, A. and Palomo, A., *Composition and microstructure of alkali activated fly ash binder: Effect of the activator*. Cement and Concrete Research, 2005. **35**(10): p. 1984-1992.
13. Duxson, P.P., J.L. , *Designing precursors for geopolymer cements*. Journal of the American Ceramic Society, 2008.
14. White, C.E., Provis, J.L., Proffen, T. and van Deventer, J.S.J., *Molecular mechanisms responsible for the structural changes occurring during geopolymerization: Multiscale simulation*. AIChE Journal, 2011: p. n/a-n/a.
15. Yip, C.K., Lukey, G.C. and van Deventer, J.S.J., *The coexistence of geopolymeric gel and calcium silicate hydrate at the early stage of alkaline activation*. Cement and Concrete Research, 2005. **35**(9): p. 1688-1697.
16. Kouassi, S.S., Andji, J., Bonnet, J.P. and Rossignol, S., *Dissolution of waste glasses in high alkaline solutions*. Ceramics - Silikaty, 2010. **54**(3): p. 235-240.
17. Montes, C. and Allouche, E., *Influence of Activator solution formation on fresh and hardened properties of low-calcium fly ash geopolymer concrete*. Coal Combustion and Gasification Products Journal, 2012. **4**: p. 1-9.
18. Kupwade-Patil, K., Soto, F., Kunjumon, A., Allouche, E.N. and Mainardi, D.S., *Multi-scale modeling and experimental investigations of geopolymeric gels at elevated temperatures*. Computers & Structures, (0).
19. Benco, L., Tunega, D., Hafner, J. and Lischka, H., *Ab initio density functional theory applied to the structure and proton dynamics of clays*. Chemical Physics Letters, 2001. **333**(6): p. 479-484.
20. White, C.E., Provis, J.L., Riley, D.P., Kearley, G.J. and van Deventer, J.S.J., *What Is the Structure of Kaolinite? Reconciling Theory and Experiment*. The Journal of Physical Chemistry B, 2009. **113**(19): p. 6756-6765.
21. Morrow, C.P., Nangia, S. and Garrison, B.J., *Ab Initio Investigation of Dissolution Mechanisms in Aluminosilicate Minerals*. The Journal of Physical Chemistry A, 2009. **113**(7): p. 1343-1352.
22. Bandura, A.V., Kubicki, J.D. and Sofo, J.O., *Periodic Density Functional Theory Study of Water Adsorption on the α -Quartz (101) Surface*. The Journal of Physical Chemistry C, 2011. **115**(13): p. 5756-5766.
23. Kubicki, J.D., Blake, G.A. and Aplitz, S.E., *Ab initio calculations on aluminosilicate Q 3 species: Implications for atomic structures of mineral surfaces and dissolution mechanisms of feldspars*. American Mineralogist, 1996. **81**(7-8): p. 789-799.

24. White, C.E., Provis, J.L., Proffen, T., Riley, D.P. and van Deventer, J.S.J., *Combining density functional theory (DFT) and pair distribution function (PDF) analysis to solve the structure of metastable materials: the case of metakaolin*. Physical Chemistry Chemical Physics, 2010. **12**(13): p. 3239-3245.
25. White, C.E., Provis, J.L., Gordon, L.E., Riley, D.P., Proffen, T. and van Deventer, J.S.J., *Effect of Temperature on the Local Structure of Kaolinite Intercalated with Potassium Acetate*. Chemistry of Materials, 2010. **23**(2): p. 188-199.
26. White, C.E., Provis, J.L., Proffen, T., Riley, D.P. and van Deventer, J.S.J., *Density Functional Modeling of the Local Structure of Kaolinite Subjected to Thermal Dehydroxylation*. The Journal of Physical Chemistry A, 2010. **114**(14): p. 4988-4996.
27. Xu, H. and Van Deventer, J.S.J., *Ab initio calculations on the five-membered alumino-silicate framework rings model: implications for dissolution in alkaline solutions*. Computers & Chemistry, 2000. **24**(3-4): p. 391-404.
28. Provis, J.L. and van Deventer, J.S.J., *Geopolymerisation kinetics. 2. Reaction kinetic modelling*. Chemical Engineering Science, 2007. **62**(9): p. 2318-2329.
29. Van Hoang, V., *Composition dependence of static and dynamic heterogeneities in simulated liquid aluminum silicates*. Physical Review B, 2007. **75**(17): p. 174202.
30. *DMOL module of the Materials Studio 2003*, Accelrys, Inc: San Diego, CA.
31. Delley, B., *The conductor-like screening model for polymers and surfaces*. Mol Simul, 2006. **32**(2): p. 117-123.
32. Provis, J.L. and Van Deventer, J.S.J., *Geopolymers: Structure, Processing, Properties and Industrial Applications* 2009: Woodhead Publishing Limited.
33. Davidovits, J., *Geopolymer: Chemistry & Applications* 2008: Geopolymer Institute.
34. Davidovits, J., *Geopolymer, Green Chemistry and Sustainable Development Solutions: Proceedings of the World Congress Geopolymer 2005* 2005: Geopolymer Institute.
35. Oh, J.E., Moon, J., Oh, S.-G., Clark, S.M. and Monteiro, P.J.M., *Microstructural and compositional change of NaOH-activated high calcium fly ash by incorporating Na-aluminate and co-existence of geopolymeric gel and C-S-H(I)*. Cement and Concrete Research, 2012. **42**(5): p. 673-685.
36. Garcia-Lodeiro, I., Palomo, A., Fernández-Jiménez, A. and Macphee, D.E., *Compatibility studies between N-A-S-H and C-A-S-H gels. Study in the ternary diagram Na₂O-CaO-Al₂O₃-SiO₂-H₂O*. Cement and Concrete Research, 2011. **41**(9): p. 923-931.
37. Sholl, D. and Steckel, J.A., *Density Functional Theory: A Practical Introduction* 2009: Wiley.
38. Xu, H. and van Deventer, J.S.J., *Effect of Source Materials on Geopolymerization*. Industrial & Engineering Chemistry Research, 2003. **42**(8): p. 1698-1706.
39. Leach, A.R., *Molecular Modelling: Principles and Applications* 2001: Prentice Hall.
40. Walderhaug, O., Lander, R.H., Bjørkum, P.A., Oelkers, E.H., Bjørlykke, K. and Nadeau, P.H., *Modelling Quartz Cementation and Porosity in Reservoir Sandstones: Examples from the Norwegian Continental Shelf*, in *Quartz Cementation in Sandstones* 2009, Blackwell Publishing Ltd. p. 39-49.